arXiv:2111.13545v1 [cs.LG] 26 Nov 2021

μNCA: Texture Generation with Ultra-Compact Neural Cellular Automata

Alexander Mordvintsev* Eyvind Niklasson*
Google Research
{moralex, eyvind}@google.com



Abstract

We study the problem of example-based procedural texture synthesis using highly compact models. Given a sample image, we use differentiable programming to train a generative process, parameterised by a recurrent Neural Cellular Automata (NCA) rule. Contrary to the common belief that neural networks should be significantly over-parameterised, we demonstrate that our model architecture and training procedure allows for representing complex texture patterns using just a few hundred learned parameters, making their expressivity comparable to hand-engineered procedural texture generating programs. The smallest models from the proposed μNCA family scale down to 68 parameters. When using quantisation to one byte per parameter, proposed models can be shrunk to a size range between 588 and 68 bytes. Implementation of a texture generator that uses these parameters to produce images is possible with just a few lines of GLSL[1] or C code.

1. Introduction

Finding the shortest program to implement a desired behaviour has been of interest both in academic literature and in general computing for almost as long as general purpose computing has been available to the public. Algorithmic information theory defines Kolmogorov complexity [17, 42] as the shortest computer program generating a certain output. There exist parallels to the neighbouring fields of compression and information theory, which handle the more specific instance of transmitting information using the fewest number of bits. Outside academia, work in the demo-scene [41] has established a long tradition of encoding complex geometries and rendering algorithms into extremely short programmatic code and small compiled binaries. Likewise, the practice of code-golf - implementing a specified algorithm in the shortest length of source code - is a well recognized form of competition, with worldwide tournaments often involving very creative uses of language constructs and compiler features [40]. However, the interest in expressing an algorithm in the shortest form possible is at odds with deep learning approaches du jour, where the trend is towards ever larger models and over-parameterisation [6, 25].

Texture synthesis is usually described as algorithmic generation of new images that express perceptual similarity to a provided texture sample. The most successful non-parametric methods rely on copying target image patches or pixels into the image being generated [11, 18]. In recent years, methods relying on gradient-based optimization of image pixels to match target image statistics in a

* Contributed equally.

[1] Interactive WebGL implementations of our NCA rules are available on ShaderToy: NCA-68, NCA-588

pre-trained neural network have become common [12, 14]. These methods have been extended to optimising the parameters of a feed-forward neural network acting as a generator, transforming a noise vector into images similar to the target texture [20, 38]. Such feed-forward models can be seen as learned parametric procedural texture generators, typically having $10^5 - 10^6$ parameters. Such a large parameter space reflects the observation that neural network training achieves best results in the overparameterised regime [4, 25].

In parallel, the computer graphics community has made great progress in building tools for procedural texture generation, allowing artists and designers to creatively combine various primitives into pipelines producing high fidelity textures and materials. Procedural materials have a number of attractive properties, such as efficient sampling and compactness of the underlying representations. The expressiveness of algorithmic texture generators is hard to match: sometimes it takes an experienced programmer just a few hundred characters of OpenGL Shading Language (GLSL) code to create a complex world on a computer screen [9, 10]

2. Related Work

2.1. Texture Synthesis

There exist a few works that attempt to automatically design compact image generators given an image sample. A notable example is work [31] by Craig Reynolds, who used genetic algorithms (based on the work by Karl Sims [34]) driven by human evaluators to produce texture patches that would be unnoticeable on a given background. Some success was also achieved with describing a texture by a relatively small number of statistical parameters (*e.g.* [30] uses 710), and synthesising images that match these parameters. Later these ideas were combined with neural network based features to differentiably tune parameters of predefined procedural texture generators to match the provided texture samples [32].

2.2. Neural Cellular Automata

Cellular Automata (CA) have been long known to possess the capacity to act as powerful texture generators [37, 43]. There is even evidence for cellular automata-like processes generating the skin textures of certain animals [22].

Recent work [26] demonstrated a method to learn texture-generating CA given individual image samples. In this method, the CA update rule is parameterised with a comparatively small neural network. The output of the CA is fed into a pre-trained discriminative network. The rules are then differentiably optimised so as to induce feature statistics in certain layers in the discriminative network matching the target statistics of the desired sample image. This model was termed Texture Neural Cellular Automata (TNCA).

In this work we extend the TNCA line of research through reduction - we study the limits of expressivity of TNCA as they are made more compact. We demonstrate that TNCA having just a few hundred learned parameters (our smallest model has just 68), instead of several thousands, can be trained to generate a wide range of textures. The parameters of the NCA update rule can be seen as a very compact texture representation, and training such models is a form of texture compression.

2.3. Optimal Transport

Optimal transport describes the task of transforming one distribution to another, while minimising the so-called "earth movers distance". Optimal transport has its roots in the problem setting of finding the optimal redistribution of troops from their current locations to front-line locations, but has since been generalised to transporting a given distribution of points in any space to another distribution under an arbitrary transport cost-matrix.

Traditionally the problem has been computationally complex, $O(N^4)$ in the number of points. However, recent work [8] by Cuturi et. al have derived a more efficient, and differentiable, algorithm based on the Sinkhorn algorithm, making feasible a whole new set of applications for optimal transport theory [29]. The problem setting of computing divergence between two distributions, and differentiating through such a divergence appears in many sub-fields of machine learning [27] [36].

3. Training Ultra-Compact Neural CAs

3.1. Ultra-Compact Neural CA models (μNCA)

Our texture generator model is inspired by the Neural CA model from [24, 26]. It operates on a regular grid where each cell is represented using a vector of scalar values, the first 3 of which are interpreted as the R, G and B color channels, respectively. Similarly, we use differentiable optimization to find a CA rule whose repeated application in each cell on the grid produces the desired texture. The inputs to the update rule on a given cell are only the state of the cell itself and information about its immediate neighbourhood, obtained by convolving a set of fixed filters over the states of surrounding cells. At first glance, this approach may seem contrived or artificially constrained, but it enables surprising and noteworthy learned procedural behaviour. The models used in the works [24, 26] are already relatively small in size as compared to contemporary work in deep learning. Comprised of just 5856 parameters they are capable of producing a large variety of textures. Authors also demonstrate these models to be tolerant to 8-bit quantization of weights and activations.

We propose a modified version of the texture NCA model from [26], which we term μNCA. This model can be summarized in a following set of equations:

$$\mathbf{s} = [s^0 = R, s^1 = G, s^2 = B, s^3, ..., s^{C-1}] \quad (1)$$

$$K = [\underbrace{K_{lap} \cdots}_{\times N_{lap}}, \underbrace{K_x \cdots}_{\times N_x}, \underbrace{K_y \cdots}_{\times N_y}] \quad (2)$$

$$\mathbf{p} = concat(\mathbf{s}, [K_i * s^i]_{i \in 0..C-1}) \quad (3)$$

$$\mathbf{y} = concat(\mathbf{p}, abs(\mathbf{p})) \quad (4)$$

$$\mathbf{s}_{next} = \mathbf{s} + \mathbf{y}\mathbf{W}_{C \cdot 4 \times C} + \mathbf{b} \quad (5)$$

Like TNCA, our μNCA operates on a uniform grid, where the state of each cell is represented by a C-dimentional vector $\mathbf{s}$, and its first three components are visible as RGB colors (Eq. (1)), $\mathbf{p}$ represents the perception vector and $\mathbf{s}_{next}$ is the updated cell state after one iteration. The following modifications were made to compress the model, making its memory footprint smaller and evaluation more computationally efficient:

- The original texture NCA computed a "perception vector" $\mathbf{p}$ by applying a set of convolutional filters (K_{lap}, K_x, K_y) to each channel of the cell state. We use only a single filter per channel (repeating filters to cover all channels, see table 1), thus reducing the dimensionality of $\mathbf{p}$ to be the same as the number of channels. We also concatenate the filtered values with $\mathbf{s}$ so that cells continue to have full access to their own state (Eqs. (2) and (3)).

$$\underset{K_{lap}}{\begin{bmatrix} 1 & 2 & 1 \\ 2 & -12 & 2 \\ 1 & 2 & 1 \end{bmatrix}} \quad \underset{K_x}{\begin{bmatrix} -1 & 0 & 1 \\ -2 & 0 & 2 \\ -1 & 0 & 1 \end{bmatrix}} \quad \underset{K_y}{\begin{bmatrix} -1 & -2 & -1 \\ 0 & 0 & 0 \\ 1 & 2 & 1 \end{bmatrix}}$$

- We introduce non-linearity into the model by expanding the perception vector, concatenating it with a vector consisting of the corresponding absolute values of $\mathbf{p}$ (Eq. (4)). This can be seen as variant of PReLU non-linearity [13], where both slopes for negative and positive input values can be learned [2].

- We remove the latent 1x1 convolution layer from the model. The cell state updates are instead directly computed with a single matrix multiplication (in practice implemented as 1x1 convolution). All learned parameters are represented by the weight matrix $\mathbf{W}$ and the bias vector $\mathbf{b}$. Total number of parameters equals to $4 \cdot C^2 + C$, where $C = N_{lap} + N_x + N_y$. Varying $N_{\{lap,x,y\}}$ we define a family NCA of models of different expressive power. Please refer to the Tab. 1 for the specific values used in our experiments.

[2] for instance, consider ReLU, which can be represented using the linear combination: $relu(x) = (x + |x|)/2$

- Texture NCAs as described in [26] use stochastic updates to introduce randomness into the system as well as to break symmetry between cells. In this work we removed stochastic updates from the CA rule for simplicity. In order to break the symmetry, and to introduce stochasticity in the procedural generation, we initialize the grid with uniformly distributed random values in $[-0.5, 0.5]$.

3.2. Optimal Transport as a Differentiable Texture Similarity Function

In order to use differentiable optimisation to synthesize textures or to train texture generators, one must define an objective function that would measure the perceptual proximity of the current solution to the target example. The naive pixel-wise difference is not appropriate because by the nature of the problem we are looking to produce novel samples of the target texture, not pixel-perfect copies. Over time, a number of differentiable texture similarity functions have been proposed in literature.

Most contemporary texture generation methods rely on pre-trained convolutional neural networks to extract target image features [12] (sometimes referred to as "statistics"), and try to match the distribution of these features between the image under generation and the target texture. A prominent example is the work [12], which used an ImageNet-pretrained VGG feature extractor [33] and the difference between the feature channel covariance matrices as the loss. Subsequent works have explored other approaches to computing the discrepancy between feature distributions, more recently based on optimal transportation theory [14, 15].

There are significant drawbacks to VGG-based feature extractors that constrain their applicability. Models using them as feature extractors are unlikely to work well on out-of-distribution data (with regards to the distribution of data the feature extractor was trained on). Similarly, models are primarily constrained to RGB images, preventing the synthesis of textures with additional data encoded in the other channels, such as surface normals, roughness, or opacity. Pre-deep learning methods, such as using texture image patches partially offset many of these issues and may be used in the place of features extracted from deep neural networks [15, 39].

In this work we propose a differentiable texture similarity function we term OTT-Loss, combining ideas from [15, 39]. Our proposed method represents a target texture as a collection of image patches extracted from the image at various scales. A procedure that allows matching the distribution of patches between a source and a target in a differentiable fashion allows for any differentiable model to be used a generator. In practice, we use recent advances in optimal transport theory - specifically the sinkhorn iteration algorithm [8] to calculate the cost of optimal re-allocation

of patches between the output of the μNCA and the distribution of patches from the chosen target texture.

In this work we extract all possible $K \times K$ patches from the levels of the Gaussian pyramid, computed for the target image. We observed that local contrast enhancement is beneficial for the μNCA training convergence speed. To achieve it we do the sharpening of the pyramid levels before extracting the patches using the formula:

$$sharpen(I) = I + 2(I - G_{5\times5} * I)$$

where $G_{5\times5}$ is a Gaussian blur kernel.

We flatten each patch into a one-dimensional vector, effectively placing it in a feature space of all possible K sized patches. Our feature extraction procedure is shown in Algorithm 1. We then match the induced distributions of patches in this space to patches sampled from the chosen target texture. This must be done separately at each pyramid level:

$$textureLoss(F, F_{target}) = \sum_{level} OT_\epsilon(S(F^{level}), S(F^{level}_{target}))$$

where OT_ϵ denotes the optimal transport divergence, and the function $S(F)$ stochastically subsamples a number of rows (we use 2048) from a given matrix to make the OT computation tractable.

Algorithm 1: $extractFeatures$ function

Data: Image I, N_{levels}, patch size K
Result: $[F^l]_{l\in1..N_{levels}}$
$I_1 \leftarrow I$;
for $l = 1$ **to** N_{levels} **do**
  $I_{sharp} \leftarrow sharpen(I_l)$;
  $F^l \leftarrow$ list of all $K \times K$ overlapping patches extracted from I_{sharp} ;
  $I_{l+1} \leftarrow$ downscale I_l by a factor of 2
end

3.3. Training procedure

Our training procedure (Algorithm 2) is based on the one proposed in Mordvintsev et. al with a few modifications:

- On back-propagation we apply gradient normalization after every CA step. This may be seen as a variant gradient clipping [28], a standard practice to prevent exploding or vanishing gradients in RNN training.
- We inject seed states into training batches every $seed_rate$ training steps, rather than at every step. This allows CA to witness longer CA evolution sequences during training, which results in better long-term pattern quality and stability. The expected number of CA steps seen during training becomes $N_{batch} * N_{steps} * seed_rate$.
- Overflow loss, $L_{overflow}$ (see 2), to keep latent channels in $[-1, 1]$. This stabilises training by preventing drift in latent channels and aids in post-training quantisation.

We keep other augmentations as introduced in [26], including gradient normalisation prior to taking the optimization step, and using a sample pool to achieve longer-time stabilisation.

Algorithm 2: Texture NCA Training

Data: Target texture image I_{target}
Result: final CA parameters θ
$\theta \leftarrow$ init CA parameters ;
$opt \leftarrow$ init Adam optimizer;
$pool \leftarrow$ init state pool with N_{pool} seed states;
$F_{target} \leftarrow extractFeatures(I_{target})$;
for $step = 1$ **to** N_{train} **do**
  $x \leftarrow$ sample N_{batch} states from $pool$;
  if $step \bmod seed_rate = 0$ **then**
    $x[0] \leftarrow$ random seed state
  end
  for $i = 1$ **to** N_{steps} **do**
    $x = ca(x)$;
    $x = norm_grad(x)$
  end
  $I_{gen} \leftarrow$ extract RGB-channels from x;
  $F_{gen} \leftarrow extractFeatures(I_{gen})$;
  $L_{texture} \leftarrow textureLoss(F_{gen}, F_{target})$;
  $L_{overflow} \leftarrow \sum |x - clip_{[-1,1]}(x)|$;
  $L = L_{texture} + L_{overflow}$;
  $\nabla L_\theta \leftarrow$ use back-propagation through CA steps to computes the gradient of L;
  $G_{normed} \leftarrow \nabla L_\theta / ||\nabla L_\theta||_2$;
  $\theta \leftarrow opt.update(G_{normed})$;
  place final grid states x back to the $pool$;
end

4. Experiments

4.1. Datasets

We demonstrate qualitative performance on an assortment of textures sourced from several datasets. Most of the datasets were released in tandem with texture-generation methods, and have over time been re-used and mixed across different publications, making proper attribution difficult. The textures we use in this work are curated from the following datasets:

- Images collected by Portilla and Simoncelli for their work on texture synthesis [30]. In turn, these include 'personal photographs' scanned by the authors,

as well as the MIT Vision Texture database [3] and scanned images from Textures: A Photographic Album for Artists and Designers [5].

- Images release together with *Appearance-space texture synthesis* [19].
- The Describable Textures Dataset [7].

4.2. Results

The opening figure shows curated samples of the μNCA trained on various textures, some natural and some artificial, for different model sizes of the compact NCA. The number of parameters and filter configuration for each model size is listed in 1. Notice that the largest model is 588 parameters, or about 2,352 bytes in size, while the smallest model is just 272 bytes. Thorough experimentation with quantisation of the models to just one byte per parameter showed no evidence of degradation in quality. We release a reference shader-based implementation of μNCA inference which operates on the quantised models. The quantisation brings the size of models down to between 588 bytes and 68 bytes. For complex textures involving lots of fine detail without much regularity, the model degrades gracefully with size, in most cases continuing to capture macroscopic detail (colour distributions and larger features). Simpler and more regular patterns, such as the zebra stripes, are captured equally well by both the small and large models.

4.2.1 Quantitative evaluation

Quantitative comparison of a synthesized texture with the intended target is an ongoing area of research [21], in no small part due to the open-ended definition of the texture synthesis task itself. Approaches from the family of Fréchet inception distances (”FID score”), commonly used in other image-generation settings, are not applicable, in part because the objective of μNCA is not to produce a competitive natural image generator, and also because most baselines for texture-synthesis, such as TNCA, utilize Gatys et. al approach of matching feature statistics during training. Thus, FID would make the optimization objective and evaluation criteria one and the same (albeit with a different convolutional architecture). Other works [15, 19, 30] in the field likewise present scant quantitative evaluation, and instead focus on qualitative samples and analysis.

4.3. Ablations

We qualitatively study the ablation of two elements of our proposed training procedure - gradient normalisation and overflow loss. Samples of two patterns under these ablations can be seen in 3. In addition to the perceptual degradation in quality, the training process exhibited instabilities under both ablations, with frequent explosions in state space or in gradient space. Such instabilities are exacerbated by use of the training sample pool, where corruption of the states involved in a one training iteration may be re-sampled at later training iterations.

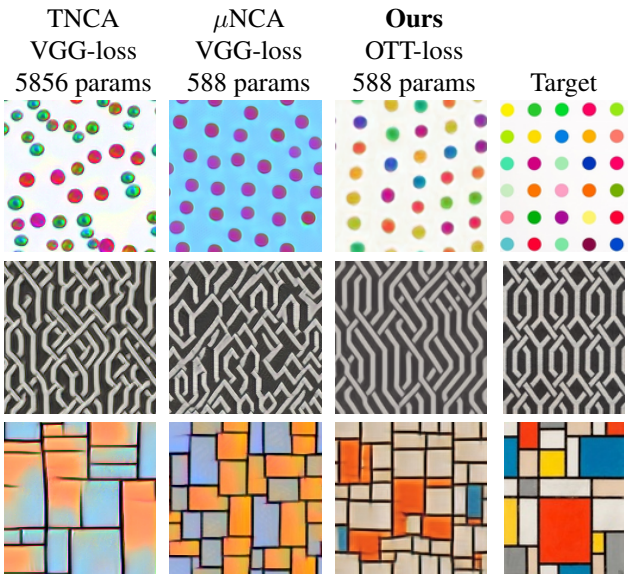


Figure 1. Comparison with original TNCA loss and architecture (VGG-loss and 5856 parameters) and with μNCA trained using VGG-loss (588 parameters). A persistent problem with matching image statistics in a pre-trained convolutional network is drift in the colour channels and inaccurate colour reproduction, as seen here. In TNCA, it appears this problem is somewhat alleviated by the relatively higher parameter count - applying VGG-loss to the 588 parameter μNCA degrades the quality of the produced patterns in most cases. OTT-loss is unbiased in colour space, as each primary colour channel is simply a dimension in the patch feature space and treated equally under optimal transport divergence. We note that even spatially complex patterns, such as the weave, are still reproduced well by the μNCA, despite having far fewer parameters than TNCA.

4.4. Optimal Transport Loss Control

The use of patches and an Optimal Transport based loss affords more fine grained control over the texture similarity metric than traditional feature-statistic matching based methods. The target texture is encoded as a distribution of image patches; tuning the size and nature of these patches provides intuitive ”control knobs” for the training process. For instance, the effective size of the largest patch at the highest level of the pyramid ($K * 2^{N_{levels}-1}$) approximately determines the size of the largest features in the target image that will synthesized in the source image under generation. Note that this is only an approximate limit; the overlap between patches can still result in larger visual features being correctly synthesized, but more often than not patches will be recombined in a locally-consistent, globally-inconsistent

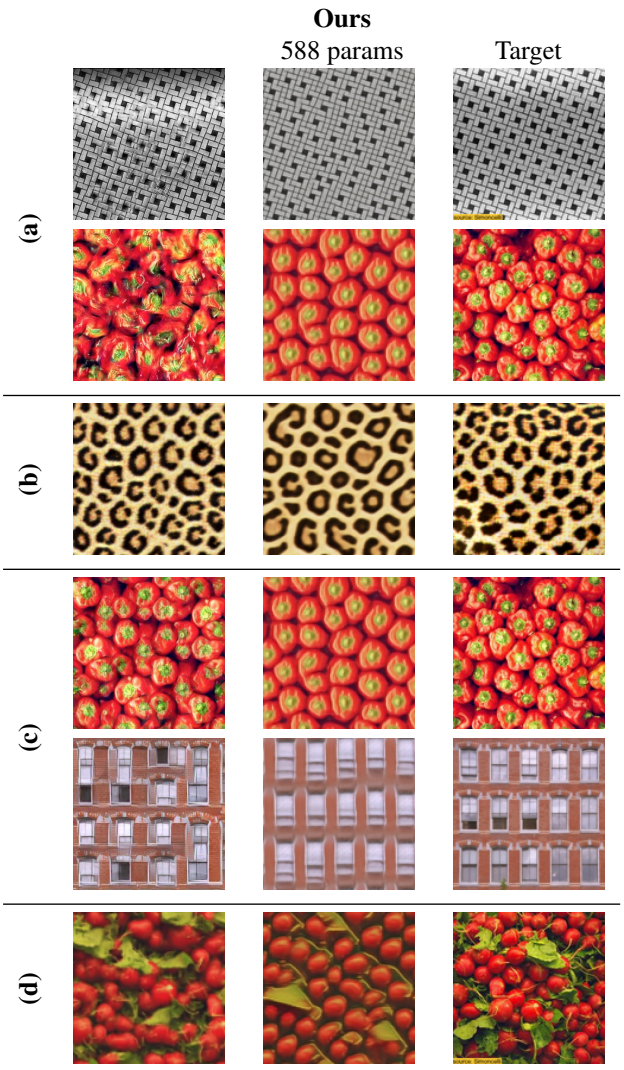


Figure 2. Comparison of μNCA with different well-known texture synthesis approaches. In order, **a)** *(710 params)* Portilla and Simoncelli's [30] approach based on matching hand-defined pixel statistics, **b)** *(parameter-free)* Hugues Hoppe's [19] work on constructing and utilizing an "appearance space" to aid in the selection of patches from the target image, **c)** *(approx. 65k params)* Ulyanov et al's work [38] on using pre-trained convolutional networks as feature-extractors to differentiably train a generator network, **d)** *(approx. 65k params)* Houdard et al's work [16] on using optimal transport to match feature statistics in images, in order to backpropagate into a generator network (as in (c)). We note they describe their generator network, TexNet, as "small", at 65k parameters.

manner. See figure 4 to see the effects of different patch sizes.

(N_{lap}, N_x, N_y)	C	N_{params}
(2, 1, 1)	4	68
(2, 2, 2)	6	150
(4, 2, 2)	8	264
(4, 4, 4)	12	588

Table 1. μNCA filter configurations used in the experiments.

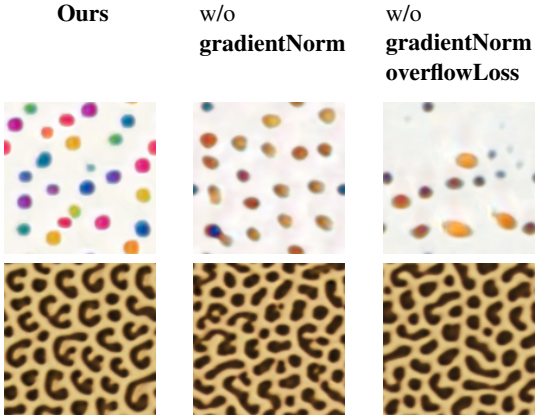


Figure 3. Qualitative ablation results for training augmentations introduced. In addition to degradation in the quality of the converged pattern, lack of these augmentations often leads to exploding states, or exploding gradients.

4.5. μNCA Dynamics

The inherent nature of μNCA as iterative models prevents static visualisations of their states from fully capturing their behaviour. We suggest readers interact with sample μNCA models, implemented as shader programs, available here: NCA-68, NCA-588. Additionally, we provide code to train μNCA in the supplementary materials.

5. Discussion

5.1. Procedural Generation

We hypothesize that the extreme constraint on the number of parameters prevents overfitting or even learning any significant section of the bitmap verbatim (indeed, the target sample image bitmaps themselves are approximately $128*128*3 = 49152$ bytes, as compared to 68 bytes in our smallest model). Similarly, see figure 5 to see a comparison to a traditional image encoding algorithm, JPEG, with the lowest quality setting at approximately 500 bytes versus 264 bytes in our smallest quantised model, albeit with some overhead for the JPEG file format. Other formats, such as JPEG-XL (JXL), allow for far more compact representations, and as a result there is a field of "JXL art" [1] focusing on writing minimal valid JXL files on the order of tens of bytes. At first glance, these hand-engineered JXL

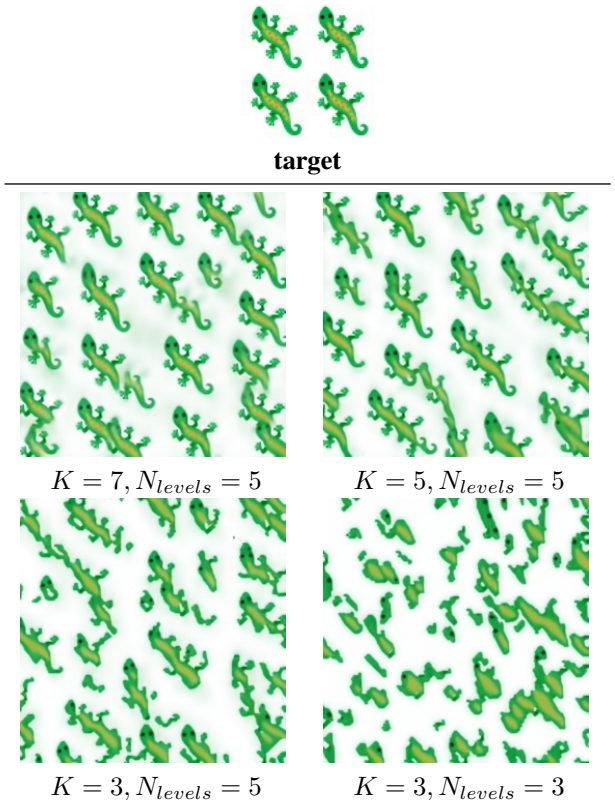


Figure 4. **Pixel-optimisation** using OTT-Loss using Adam with $1e-3$ learning rate for 200 iterations. *Note that μNCA are unable to learn this target image; we intend this figure to demonstrate the "control knobs" made available by OTT-Loss*. Larger patches and more levels result in consistent macroscopic detail, such as the structure of the body, while smaller patches and fewer levels produce an image with consistent microscopic detail but lacking all larger-scale coherence, resulting in an abundance of lizard eyes and other immediately local features, but no discernible structure to their composition.

files appear to match the expressivity of μNCA. However, the underlying model of μNCA could conceivable be implemented in at most hundreds of lines of standard C code [23], while the JPEG-XL reference library [2] is composed of hundreds of thousands of lines.

We posit that the learned parameters represent a near-minimal procedural program that satisfies the desired behaviour (to stochastically generate a perceptually similar texture to a given sample image), and that the model must learn to exploit any regularities in the pattern to achieve this task. Hand-engineered procedural texture generators are often written in an extremely compact fashion, but still rely on extensive graphics libraries. We emphasize that most of the generative process, or the procedural program, for a learned texture is effectively entirely encoded in the parameters; the underlying architecture used for μNCA is not complex.

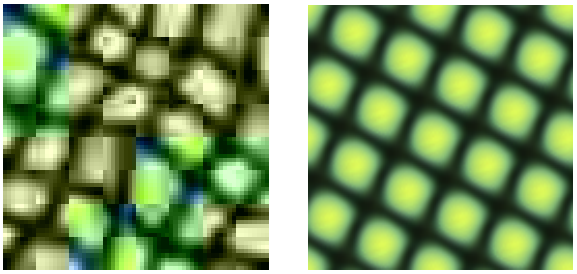


Figure 5. Comparison of a JPEG encoded image and the output of a μNCA rule with fewer than half the number of bytes. μNCA make use of regularity in patterns to learn procedural generation.

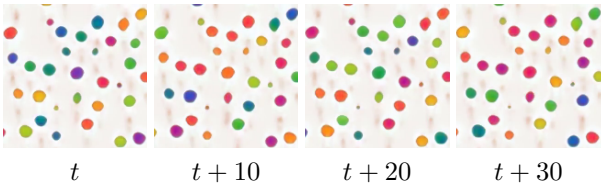


Figure 6. Four samples, each 10 steps apart, after pattern convergence, from a μNCA trained on a polka dot pattern. Occasionally, the μNCA converges to the remarkable procedural solution of synthesizing a number of dots, then having each dot oscillate through the target colours, while ensuring they are not in sync in order to produce the desired target distribution of colours among the dots at any given time-step. Closer inspection reveals the dots oscillate across colours in the same order.

We find further evidence for this hypothesis when qualitatively observing the model's behaviour during iteration. When the model is trained on a "polka dot" pattern 6, which features regularly spaced dots of different colours against a white background, we observe that on occasion the μNCA with 8 channels (280 parameters) will converge to a solution where the coloured dots oscillate in colour, as opposed to simply generating an image with several multi-coloured dots spatially distributed across the image in different, fixed, colours. We believe this behaviour is indicative that the solution space of μNCA is the space of possible procedural programs, in contrast to some parameterisation of different statistics of the image. Designing a program where the output is a polka dot pattern in different colours, with the constraint that the program's output must be a valid "polka dot" pattern at any given step after some period of convergence, certainly admits the non-intuitive solution of producing bubbles of oscillating colour.

5.2. Limitations

The method outlined here, like the originally proposed NCA, learns a complete generative model per target texture. This is comparable to single-image CPPNs and other work

that uses neural networks to encode single data points [35] [38]. It is conceivable that knowledge could be shared between different models operating on the same space of natural images, and thus a current limitation which may need to be explored further is the sharing of parameters between models. However, the focus of this work on ultra-compact models narrowed the scope of experiments to those involving single images per model.

The texture samples produced by μNCA and the underlying work TNCA do not produce images indistinguishable from images from the natural world. The models perform significantly better on regular patterns (especially artifically produces ones, such as grids or other repeated features). The distinguishing features of μNCA are their extremely compact nature and robustness inherent to their architecture (embarrasingly parallel and highly fault-tolerant).

References

[1] JPEG XL art. https://sneyers.info/jxl/art/. Accessed: 2021-11-17. 6

[2] libjxl: JPEG XL image format reference implementation. 7

[3] MIT vision texture database. 5

[4] Mikhail Belkin, Daniel Hsu, Siyuan Ma, and Soumik Mandal. Reconciling modern machine-learning practice and the classical bias-variance trade-off. *Proc. Natl. Acad. Sci. U. S. A.*, 116(32):15849–15854, Aug. 2019. 2

[5] Phil Brodatz. *Textures: A Photographic Album for Artists and Designers*. Peter Smith Publisher, Incorporated, June 1981. 5

[6] Tom B Brown, Benjamin Mann, Nick Ryder, Melanie Subbiah, Jared Kaplan, Prafulla Dhariwal, Arvind Neelakantan, Pranav Shyam, Girish Sastry, Amanda Askell, Sandhini Agarwal, Ariel Herbert-Voss, Gretchen Krueger, Tom Henighan, Rewon Child, Aditya Ramesh, Daniel M Ziegler, Jeffrey Wu, Clemens Winter, Christopher Hesse, Mark Chen, Eric Sigler, Mateusz Litwin, Scott Gray, Benjamin Chess, Jack Clark, Christopher Berner, Sam McCandlish, Alec Radford, Ilya Sutskever, and Dario Amodei. Language models are Few-Shot learners. May 2020. 1

[7] M. Cimpoi, S. Maji, I. Kokkinos, S. Mohamed, , and A. Vedaldi. Describing textures in the wild. In *Proceedings of the IEEE Conf. on Computer Vision and Pattern Recognition (CVPR)*, 2014. 5

[8] Marco Cuturi. Sinkhorn distances: Lightspeed computation of optimal transportation distances. June 2013. 2, 3

[9] Junyu Dong, Jun Liu, Kang Yao, Mike Chantler, Lin Qi, Hui Yu, and Muwei Jian. Survey of procedural methods for Two-Dimensional texture generation. *Sensors*, 20(4), Feb. 2020. 2

[10] D Ebert, F K Musgrave, D Peachey, K Perlin, and Steven Worley. Texturing and modeling: a procedural approach. *Choice*, 32(09):32–5129–32–5129, May 1995. 2

[11] Alexei A Efros and Thomas K Leung. Texture synthesis by non-parametric sampling. 1

[12] Leon A Gatys, Alexander S Ecker, and Matthias Bethge. Texture synthesis using convolutional neural networks. May 2015. 2, 3

[13] Kaiming He, Xiangyu Zhang, Shaoqing Ren, and Jian Sun. Delving deep into rectifiers: Surpassing Human-Level performance on ImageNet classification. Feb. 2015. 3

[14] Heitz, Vanhoey, Chambon, and Belcour. A sliced wasserstein loss for neural texture synthesis. In *2021 IEEE/CVF Conference on Computer Vision and Pattern Recognition (CVPR)*, volume 0, pages 9407–9415, June 2021. 2, 3

[15] Antoine Houdard, Arthur Leclaire, Nicolas Papadakis, and Julien Rabin. A generative model for texture synthesis based on optimal transport between feature distributions. June 2020. 3, 5

[16] Antoine Houdard, Arthur Leclaire, Nicolas Papadakis, and Julien Rabin. A generative model for texture synthesis based on optimal transport between feature distributions. June 2020. 6

[17] A N Kolmogorov. On tables of random numbers. *Theor. Comput. Sci.*, 207(2):387–395, Nov. 1998. 1

[18] Sylvain Lefebvre and Hugues Hoppe. Appearance-space texture synthesis. In *ACM SIGGRAPH 2006 Papers on - SIGGRAPH '06*, New York, New York, USA, 2006. ACM Press. 1

[19] Sylvain Lefebvre and Hugues Hoppe. Appearance-space texture synthesis. *ACM Trans. Graph.*, 25(3):541–548, July 2006. 5, 6

[20] Yijun Li, Chen Fang, Jimei Yang, Zhaowen Wang, Xin Lu, and Ming-Hsuan Yang. Diversified texture synthesis with feed-forward networks. In *2017 IEEE Conference on Computer Vision and Pattern Recognition (CVPR)*. IEEE, July 2017. 2

[21] Wen-Chieh Lin, J Hays, Chenyu Wu, Yanxi Liu, and V Kwatra. Quantitative evaluation of near regular texture synthesis algorithms. In *2006 IEEE Computer Society Conference on Computer Vision and Pattern Recognition (CVPR'06)*, volume 1, pages 427–434, June 2006. 5

[22] Liana Manukyan, Sophie A Montandon, Anamarija Fofonjka, Stanislav Smirnov, and Michel C Milinkovitch. A living mesoscopic cellular automaton made of skin scales. *Nature*, 544(7649):173–179, Apr. 2017. 2

[23] Alexander Mordvintsev. deepdream_c: Minimalistic DeepDream with C89. 7

[24] Alexander Mordvintsev, Eyvind Niklasson, and Ettore Randazzo. Texture generation with neural cellular automata. May 2021. 2

[25] Preetum Nakkiran, Gal Kaplun, Yamini Bansal, Tristan Yang, Boaz Barak, and Ilya Sutskever. Deep double descent: Where bigger models and more data hurt. Dec. 2019. 1, 2

[26] Eyvind Niklasson, Alexander Mordvintsev, Ettore Randazzo, and Michael Levin. Self-Organising textures. *Distill*, 6(2), Feb. 2021. 2, 3, 4

[27] Derek Onken, Samy Wu Fung, Xingjian Li, and Lars Ruthotto. OT-Flow: Fast and accurate continuous normalizing flows via optimal transport. May 2020. 2

[28] Razvan Pascanu, Tomas Mikolov, and Yoshua Bengio. On the difficulty of training recurrent neural networks. Nov. 2012. 4

[29] Gabriel Peyré and Marco Cuturi. Computational optimal transport. Mar. 2018. 2

[30] Javier Portilla and Eero P Simoncelli. A parametric texture model based on joint statistics of complex wavelet coefficients. http://www.cns.nyu.edu/pub/eero/portilla99-reprint.pdf, 2000. Accessed: 2021-11-11. 2, 4, 5, 6

[31] Craig Reynolds. Interactive evolution of camouflage. *Artif. Life*, 17(2):123–136, Mar. 2011. 2

[32] Liang Shi, Beichen Li, Miloš Hašan, Kalyan Sunkavalli, Tamy Boubekeur, Radomir Mech, and Wojciech Matusik. Match: Differentiable material graphs for procedural material capture. *ACM Trans. Graph.*, 39(6):1–15, Dec. 2020. 2

[33] Karen Simonyan and Andrew Zisserman. Very deep convolutional networks for Large-Scale image recognition. Sept. 2014. 3

[34] Karl Sims. Artificial evolution for computer graphics. *SIGGRAPH Comput. Graph.*, 25(4):319–328, July 1991. 2

[35] Kenneth O Stanley. Compositional pattern producing networks: A novel abstraction of development. *Genet. Program. Evolvable Mach.*, 8(2):131–162, June 2007. 8

[36] Luis Caicedo Torres, Luiz Manella Pereira, and M Hadi Amini. A survey on optimal transport for machine learning: Theory and applications. June 2021. 2

[37] Greg Turk. Generating textures on arbitrary surfaces using reaction-diffusion. In *Proceedings of the 18th annual conference on Computer graphics and interactive techniques - SIGGRAPH '91*, New York, New York, USA, 1991. ACM Press. 2

[38] Dmitry Ulyanov, Andrea Vedaldi, and Victor Lempitsky. Improved texture networks: Maximizing quality and diversity in feed-forward stylization and texture synthesis. In *2017 IEEE Conference on Computer Vision and Pattern Recognition (CVPR)*. IEEE, July 2017. 2, 6, 8

[39] Ryan Webster. Innovative non-parametric texture synthesis via patch permutations. Jan. 2018. 3

[40] Wikipedia contributors. Code golf. https://en.wikipedia.org/wiki/Code_golf, Sept. 2021. Accessed: 2021-11-16. 1

[41] Wikipedia contributors. Demoscene. https://en.wikipedia.org/wiki/Demoscene, Nov. 2021. Accessed: 2021-11-16. 1

[42] Wikipedia contributors. Kolmogorov complexity. https://en.wikipedia.org/wiki/Kolmogorov_complexity, Nov. 2021. Accessed: 2021-11-16. 1

[43] Andrew Witkin and Michael Kass. Reaction-diffusion textures. In *Proceedings of the 18th annual conference on Computer graphics and interactive techniques - SIGGRAPH '91*, New York, New York, USA, 1991. ACM Press. 2